THE ASTROPHYSICAL JOURNAL, 296:390–398, 1985 September 15


# THE KINEMATICS AND INTERNAL DYNAMICS OF PLANETARY NEBULAE IN THE SMALL MAGELLANIC CLOUD

MICHAEL A. DOPITA, HOLLAND C. FORD,[2] CATHERINE J. LAWRENCE,[1] AND B. LOUISE WEBSTER[3]

*Received 1984 December 13; accepted 1985 March 15*

## ABSTRACT

We have investigated the radial velocity and internal motions of 44 Small Magellanic Cloud (SMC) planetary nebulae (PN) in the [O III] 5007 Å emission line at a resolution of 12 km s$^{-1}$ (FWHM). From a kinematical viewpoint, the PNs form an unstructured spheroidal population apparently associated with the Bar with centroid at $\alpha 00^h 49^m 39^s$, $\delta - 73°30'$ (1950) and with a mean radial velocity, $V_{GSR}$, of $-17$ km s$^{-1}$. Their velocity dispersion implies a mass of $9 \times 10^8$ $M_\odot$ within a radius of 3 kpc of the centroid. The H I is known to show a bimodal velocity structure. These PNs, which form a population of age $\gtrsim 10^8$ yr, appear to be loosely associated with the lower velocity component, suggesting that the high-velocity H I structure is dynamically young. These is some evidence for a younger population of rapidly expanding PNs found with intermediate radial velocities and concentrated to the north and east of the SMC which may be associated with earlier star formation in the dynamically young H I feature.

We find a remarkably good correlation between the expansion velocity and excitation class. From the selection effects operating in the sample, we argue that this may show that the mass of the white dwarf central star is the major variable influencing the expansion velocity of planetary nebulae.

*Subject headings:* galaxies: internal motions — galaxies: Magellanic Clouds — galaxies: structure — nebulae: planetary — radial velocities — stars: white dwarfs

## I. INTRODUCTION

Despite many years of study, our understanding of the internal dynamics of planetary nebulae (PNs) is somewhat rudimentary. For example, no clear consensus has yet emerged as to the evolutionary trend of the expansion velocity in Galactic objects, Robinson, Reay, and Atherton (1982) arguing that high- and low-mass PNs have different expansion velocity/radius relationships, whereas other authors suggest that a single relationship exists with maximum expansion velocity being reached at a radius $\sim 0.2$ pc with a slow decline to larger radius (Smith 1969; Bohuski and Smith 1974; Sabbadin and Hamzaoglu 1982). Recent papers by Sabbadin and his coworkers (Sabbadin, Bianchini, and Hamzaoglu 1984; Sabbadin *et al.* 1984) have added to both our theoretical and our observational understanding of this problem. They conclude that the best concordance with the data is obtained for a model in which the PN is a Strömgren sphere evolving into an expanding nebula which has been suddenly injected by an asymptotic giant branch (AGB) star.

We might expect that the population of PNs in the Magellanic Clouds, by furnishing us with a large luminosity-limited sample at a common distance, would enable us to learn a great deal about the dynamical evolution of such objects. This would apply, in particular, to those PNs with the more massive white dwarf nuclei which should be represented by a (rare) highly luminous population and à (more abundant) faint population of highly excited nebulae according to the theoretical evolutionary tracks (Paczyński 1971; Iben 1981).

From a kinematical viewpoint also, the Magellanic Cloud PN have a considerable interest. This is particularly true for the SMC which has a very confusing radial velocity field. In the 21 cm line of H I, a double peak structure with a velocity splitting of 30–40 km s$^{-1}$ is apparent across much of the SMC (Hindman 1967; McGee and Newton 1981; Bajaja and Loiseau 1982; Mathewson and Ford 1984). This pattern is shared by the young stars, and Ca II H and K absorption velocities are found predominantly associated with the approaching component of the H I, suggesting that this is nearer in space (Mathewson and Ford 1984). The PNs offer an older subsystem of the SMC for which accurate kinematics can be derived. If, for example, the H I kinematics is a result of tidal forces generated in a close passage of the SMC by the LMC (Murai and Fujimoto 1980), then we should not expect the PN kinematics to resemble the H I because of the different response of the gaseous and stellar components.

Until the present work, there have only been two kinematic studies (Feast 1968, who studied 13 objects; Webster 1969, who observed seven) and no study of the internal dynamics of the SMC population of planetary nebulae. Both of the kinematic studies found (with a substantially overlapping selection of objects) that the PNs fell into two velocity groups showing a poor correlation with the H I peak. In this work we present kinematical and dynamical data for 44 SMC PNs at a velocity resolution of 12 km s$^{-1}$.

## II. OBSERVATIONS AND DATA REDUCTION

### *a) Selection of Objects*

The majority of the objects we observed came from the list of Sanduleak, McConnell, and Phillips (1978) who gave a list of 28 PNs selected from objective prism material, all of which we observed. Many of these were previously known as emission nebulae from the Henize (1956) catalog, had also been found by Lindsay and Mullen (1963), and had been positively identified as PNs by Henize and Westerlund (1963). We also observed all objects given in the supplementary list of Sanduleak and Pesch (1981), but only two of these, objects 32 and

[1] Mount Stromlo and Siding Spring Observatories, Research School of Physical Sciences, Australian National University.
[2] Space Telescope Science Institute, John Hopkins University.
[3] School of Physics, University of New South Wales.

34, are bona fide PNs, the remainder being red stars without a trace of [O III] emission.

The Jacoby (1980) objects present a difficult group. Many of these are very faint and could not be firmly identified as PNs even with the AAT 3.8 m telescope at the dispersion we were using. Only for three objects (J4, J9, and J18) have data of sufficiently high quality been obtained for inclusion here.

Recently Morgan undertook a search for SMC PNs using the new high-dispersion objective prism of the UK Schmidt Telescope. A description of the equipment used, and the first identification, is given by Morgan (1984). In addition to this we have observed 10 new candidates (Morgan and Good 1985).

### b) *The Observations*

We have used two instruments and telescopes for this study. Observations made in 1983 October and November used the 1.0 m telescope operated by the Australian National University at Siding Spring Observatory. The Perkin-Elmer echelle spectrograph was used with a 79 line mm$^{-1}$ echelle grating and a 300 line mm$^{-1}$ cross disperser. This instrument gives a dispersion of 5.08 Å mm$^{-1}$ in the [O III] 5007 Å line. The detector system used was the two-dimensional Photon Counting Array (PCA) (Stapinski, Rodgers, and Ellis 1981). This uses a 25 mm ITT microchannel plate proximity focus intensifier tube with an S20 photocathode coupled to a single-stage electrostatic image tube. The photon events on the output phosphor are read out using an uncooled Fairchild CCD 221 lens coupled to the image tube assembly. After frame subtraction to remove fixed pattern noise in the chip and afterglow from previous photon events, the data are digitized and the centroid of each photon event found to give a resolution (pixel size) in the 512 K pixel external memory of 15 × 18 $\mu$m. With a slit width of 150 $\mu$m, the whole system gave a resolution (FWHM) of 11.5 km s$^{-1}$ at the [O III] 5007 Å line.

The fainter objects, and those brighter objects for which inadequate signal-to-noise ratio had been obtained from the 1.0 m observations, were observed on the nights of 1983 December 22 and 23 using the Anglo-Australian 3.9 m telescope at Siding Spring. The RGO spectrogaph was used with its 82 cm camera and a grating of 1200 lines mm$^{-1}$ operated in second order. The detector was the Image Photon Counting System (IPCS; Boksenberg 1972). The slit width of 40 $\mu$m gave system resolution (FWHM) of 11.75 km s$^{-1}$ in the [O III] 5007 Å line. The external memory was formatted to give 2040 spectral pixels × 50 spatial elements, separated by 0″.63 on the sky.

These two systems, although quite different, give quite similar performance characteristics. The RGO spectrograph system gives a somewhat better sampling of the spectrum at 0.059 Å per pixel at [O III] 5007 Å compared with 0.083 Å per pixel for the echelle system. However, the combination of wider slit and smaller image scale offered by the echelle ensures a higher light collecting power for this system under average seeing conditions. When corrected for aperture, the echelle system was found to detect an average of 1.9 times more photons than the grating system on our radial velocity standard object SMC 27. As already mentioned, the two instruments offer effectively identical velocity resolution.

The exposure time was varied to give a typical (peak) signal in the range 50–300 photons pixel$^{-1}$. However, for some of the AAT observations of the fainter Jacoby (1980) and Morgan objects, we had to be content with lower peak signal, even though wider slits (up to 80 $\mu$m) were used on some objects, degrading the resolution to 17 km s$^{-1}$.

### c) *Reduction Procedure*

Since the reduction of the two sets of observations proceeded along almost identical procedures, we describe both here. In order to remove small-scale variations of sensitivity, each observation was divided by a normalized flat field obtained each night by very long exposures of a quartz continuum lamp through the system to give a detected signal $\sim 10^4$ photons per pixel. The data were then rebinned to give a constant wavelength interval per pixel using coefficients obtained by full two-dimensional quadratic fit to arc lamp spectra. In order to minimize instrumental drifts, each nebular observation was, in general, bracketed by arc lamp exposures, and a "mean" arc lamp observation was formed by weighting each arc lamp exposure according to its proximity in time to the PN observation. With this individualized wavelength fitting, the standard deviation of the wavelength fit averaged 0.08 pixels for the 1.0 m observations and 0.05 pixels for the 3.8 m observations, corresponding to velocity errors of 0.40 km s$^{-1}$ and 0.18 km s$^{-1}$, respectively.

After wavelength linearization, spectra were reduced to one-dimensional form by summing all spatial increments having appreciable signal.

These spectra profiles were then fitted by up to four Gaussian components using the SPECTRE code (Pelat, Alloin, and Fosbury 1981). The fits to a variety of observed profiles are shown in Figure 1. For some of the brighter planetaries observed on the 1.0 m, a spurious halo exists around the [O III] 5007 Å emission line, giving rise to faint extended wings on the profile. This is caused by halation in the image tube which gives a few counts in frame subtraction, the number being critically dependent on the absolute photon rate in the line. These wings can be seen in the profile of SMC 3 (Fig. 1). Where they occur, they have been fitted by a single broad Gaussian component which was not used further in the analysis.

Essentially, the profiles fall into three classes:

1. A single Gaussian, or single Gaussian plus "spike" not appreciably shifted in wavelength from the main peak.
2. A double component structure.
3. A double component structure with a brighter single Gaussian central feature.

### d) *Accuracy*

As already mentioned, the formal error in the accuracy of the wavelength calibration is 0.40 km s$^{-1}$ and 0.18 km s$^{-1}$ for the 1.0 m and 3.8 m observations, respectively.

Two further errors can contribute to the total. The first is simply a statistical error due to the finite number of photons detected. This introduces a very small error in the radial velocity estimate, but with the signal we obtained, may introduce an error of as much as 10% in the measurement of the full width at half-maximum (FWHM). The second error applies only to the echelle. Here the slit width of 150 $\mu$m projects to 3″.9 on the sky. Under good conditions of seeing, therefore, asymmetric slit illumination effects may produce an appreciable shift in the line centroid. We estimate the maximum error from this source to be $\pm 1.5$ km s$^{-1}$ in the radial velocity and the effective instrumental resolution could vary in the range 10–12 km s$^{-1}$. Assuming that the statistical error in determining the line centroid is of the same order as the formal error in the wavelength calibration, our estimated total error in measuring radial velocities is $\pm 1.6$ km s$^{-1}$ and $\pm 0.3$ km s$^{-1}$ for the 1.0 m and 3.8 m data, respectively. These estimates are confirmed by

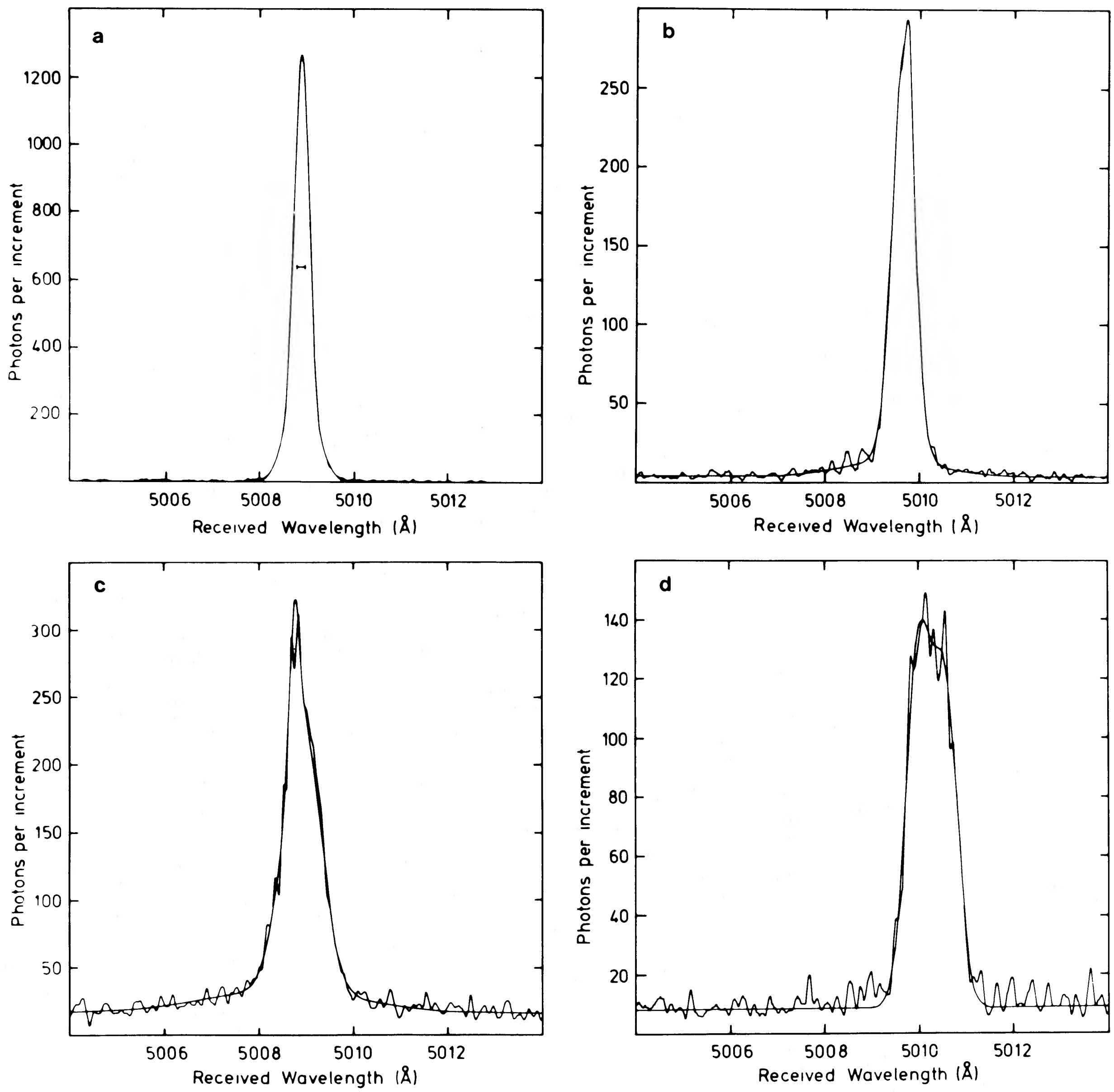


FIG. 1.—The observed line profiles and their multiple Gaussian fits for four representative cases: (*a*) SMP 27; (*b*) SMP 13; (*c*) SMP 3; (*d*) SMP 14. The full width at half-maximum of the instrumental function is represented by a horizontal bar in the SMP 27 profile, corresponding to 12 km s$^{-1}$.

independent measurements of our velocity standard in the SMC, SMP 27, given in Table 1.

On the question of accuracy, it is also of interest to compare our results with those obtained by Feast (1968) and Webster (1969). The measured heliocentric radial velocities for the objects in common are given in Table 2. We find the agreement remarkably good except for SMP 22 (N67). M. W. Feast (1985, private communication) points out that unpublished velocities measured by Dr. A. Walker also find N67 to be discrepant. A reexamination of the original plate shows that the published mean is strongly affected by a low velocity for H$\alpha$ and that, in turn, this line is probably affected by a plate flaw. Discounting the most disparate measurement in each data set, we find a mean difference of 9.1 km s$^{-1}$ between the Webster (1969) data set and our measurements, whereas for the Feast (1968) data set this difference is only 2.9 km s$^{-1}$! He is to be congratulated for a truly heroic effort with a quartz prism spectrograph, photographic plates and, in most cases, invisible objects.

## III. RESULTS

In Tables 3 and 4 we present our measured LSR radial velocities, velocity dispersions (FWHM) and expansion velocities of the SMC planetary nebulae.

The radial velocity, $V_{\rm LSR}$, is given as the area weighted mean where there is more than one component.

The velocity dispersion, $\Delta V$, of each component has been corrected for the instrumental half-width, assuming that it adds in quadrature.

The definition of an "expansion velocity" from these profiles is a somewhat arbitrary process. Those PNs which fit to a single Gaussian line profile are more likely to have roughly spherical symmetry, either filled or shell-like. In this case, the

TABLE 1

Individually Measured Radial Velocities for the Major Component of SMP 27

| $V_{LSR}$ (1.0 m) | $V_{LSR}$ (3.8 m) |
|---|---|
| 102.31 | 101.17 |
| 102.70 | 102.08 |
| 103.37 | ... |
| (104.12)[a] | ... |
| 101.57 | ... |
| 101.10 | ... |
| 98.69 | ... |
| 103.36 | ... |
| 99.17 | ... |
| 99.87 | ... |
| Mean | |
| 101.49 ± 1.51 | 101.63 ± 0.45 |

[a] Low S/N ratio; not used in mean.

gas with a high radial velocity will have a lower emission measure than the material moving predominantly in a transverse direction because of projection effects. The true expansion velocity can therefore only be determined from the full width at zero maximum. To avoid placing too much reliance on the faint wings of the profile in the presence of considerable photon noise, we have defined the expansion velocity, $V_{exp}$, as half the full width at one-tenth maximum intensity. The relationship between $V_{exp}$ and $\Delta V$ for these objects is simply $V_{exp} = 0.911\,\Delta V$.

This expansion velocity is not identical with the values for Galactic PNs. Measurements of those of the latter objects that are extended are typically made with a centrally located aperture that is much smaller than the angular diameter of the nebula, so that a double line is observed. The expansion velocity is then defined to be half the velocity difference between the peaks. If the nebula is smaller than the aperture, as for unresolved PNs or Fabry-Perot observations of larger ones, then, for a spherical symmetry, a single-peaked profile will result and Robinson, Reay, and Atherton (1982) have suggested that the half-width of the half-maximum of the profile is the quantity that corresponds most closely to the expansion velocity defined from the spit-line situation. However, this conclusion depends on the inner and outer radii of the shell and the distribution of emissivity with radius. A more complicated relation holds when the aperture size lies between the two extreme cases. It seems to us to be justified to depart from these previous less precise definitions of the expansion velocity, given that we sample all the nebulae, that we have a very uniform method of making the measurements and that we have a large number of objects observed. Should the reader prefer another definition of $V_{exp}$, it can be readily derived from the $\Delta V$ values of Tables 3 and 4.

In the case of the PNs with double and multi-component profiles given in Table 4, it is more difficult to give a satisfactory definition of expansion velocity. These PNs will tend to have a bipolar morphology, which, in the Galaxy, ranges from two ansae, or brightening on opposite sides of a shell, to a very elongated figure-of-eight structure with an intense central core. However, it is also possible that some objects may be true double-shell objects. For these objects showing only two components the following definition of $V_{exp}$ seems satisfactory:

$$V_{exp} = 0.455[\Delta V(1) + \Delta V(2)] + 0.5\,|\,V_{LSR}(1) - V_{LSR}(2)\,|\,,$$

where $V_{LSR}(1)$ and $V_{LSR}(2)$ are the radial velocities of each component and $\Delta V(1)$, $\Delta V(2)$, are the corresponding full widths at half-maximum. Such a definition, in effect, still measures half

TABLE 2

A Comparison of Radial Velocities Obtained in the Three Studies

| Object Name | | | Radial Velocity (heliocentric km s$^{-1}$) | | |
|---|---|---|---|---|---|
| SMP | N | L | This Study | Feast 1968 | Webster 1969 |
| 2 | 2 | 14 | 157.0 | 157 | ... |
| 5 | 5 | 32 | 110.2 | 109 | ... |
| 6 | 6 | 33 | 149.4 | 149 | 149 |
| 13 | 38 | 144 | 153.6 | 160 | 151 |
| 15 | 43 | 174 | 114.3 | 115 | 129 |
| 17 | 44 | 191 | 105.0 | 113 | 118 |
| 18 | 47 | 196 | 121.8 | ... | 145 |
| 20 | 54 | 289 | 99.3 | 99 | ... |
| 22 | 67 | 333 | 153.2 | 113 | ... |
| 24 | 70 | 347 | 140.8 | 148 | 159 |
| 27 | 87 | 532 | 111.3 | 117 | 109 |

TABLE 3

Velocity Data on Planetary Nebulae Fitted by a Single Gaussian

| Object[a] | Excitation Class[b] | $V_{LSR}$ | $\Delta V$ | $V_{exp}$ |
|---|---|---|---|---|
| SMP 1 ........... | 0.5 | 138.0 | 16.9 | 15.4 |
| SMP 2 ........... | 6 | 148.2 | 35.4 | 32.2 |
| SMP 5 ........... | 6–7 | 101.2 | 32.0 | 29.2 |
| SMP 8 ........... | 2–3 | 115.6 | 27.4 | 25.0 |
| SMP 9 ........... | 7–8 | 165.7 | 41.6 | 37.9 |
| SMP 10 .......... | 2 | 128.3 | 26.5 | 24.1 |
| SMP 12 .......... | 1–2 | 113.1 | 33.6 | 30.6 |
| SMP 13 .......... | 4 | 144.5 | 30.9 | 28.1 |
| SMP 15 .......... | 2–4 | 105.1 | 16.7 | 15.2 |
| SMP 16 .......... | 0 | 115.2 | 12.8 | 11.7 |
| SMP 17 .......... | 3–5 | 95.8 | 26.6 | 24.2 |
| SMP 18 .......... | 0.5 | 112.6 | 13.9 | 12.7 |
| SMP 19 .......... | 7 | 100.4 | 33.0 | 30.1 |
| SMP 20 .......... | 1–2 | 90.0 | 22.2 | 20.2 |
| SMP 21 .......... | 3 | 150.6 | 38.6 | 35.2 |
| SMP 22 .......... | 8 | 144.2 | 55.9 | 50.9 |
| SMP 23 .......... | 4 | 112.8 | 34.8 | 31.7 |
| SMP 24 .......... | 1–2 | 131.4 | 18.2 | 16.6 |
| SMP 25 .......... | 6–7 | 137.4 | 49.1 | 44.7 |
| SMP 26 .......... | 8 | 187.0 | 55.5 | 50.6 |
| SP 32 ............ | 1–2 | 159.7 | 38.6 | 35.2 |
| SP 34 ............ | 2–3 | 117.5 | 17.6 | 16.0 |
| J4 ................ | 3–7 | 139.9 | 30.9 | 28.1 |
| J9 ................ | 3–7 | 143.0 | 26.5 | 24.1 |
| J18 ............... | 3–7 | 129.6 | 20.6 | 18.8 |
| MG 13 ........... | 7–8 | 111.0 | 54.7 | 49.8 |
| MG 1 ............ | 7–8 | 173.4 | 43.3 | 39.4 |
| MG 2 ............ | 7–8 | 122.8 | 32.5 | 29.6 |
| MG 3 ............ | 7–8 | 134.0 | 31.1 | 28.3 |
| MG 4 ............ | 7–8 | 164.7 | 28.5 | 26.0 |
| MG 5 ............ | 7–8 | 173.4 | 66.8 | 60.8 |
| MG 6 ............ | 7–8 | 146.1 | 48.5 | 44.2 |
| MG 7 ............ | 7–8 | 123.8 | 15.8 | 14.4 |
| MG 10 ........... | 7–8 | 148.4 | 48.2 | 43.9 |
| MG 11 ........... | 7–8 | 164.7 | 20.2 | 18.4 |

Note.—Velocities in km s$^{-1}$.

[a] SMP = Sanduleak, McConnell, and Philip 1978; SP = Sanduleak and Pesch 1981; J = Jacoby 1980; MG = Morgan and Good 1985.

[b] Excitation class from Morgan 1984.

TABLE 4

VELOCITY DATA ON MULTICOMPONENT PLANETARY NEBULAE

| Object[a] | Excitation Class[b] | $V_{LSR}$ | $V_{exp}$ | $V_1$ | $\Delta V_1$ | $h_2$[c] | $V_2$ | $\Delta V_2$ | $h_3$[c] | $V_3$ | $\Delta V_3$ |
|---|---|---|---|---|---|---|---|---|---|---|---|
| SMP 3 ........... | 4 | 98.2 | 32.9 | 100.1 | 54.0 | 1.70 | 90.9 | 8.3 | ... | ... | ... |
| SMP 4 ........... | 4 | 141.6 | 34.6 | 143.3 | 24.7 | 0.09 | 110.5 | 15.3 | ... | ... | ... |
| SMP 6 ........... | 4 | 140.4 | {21.9, 48.4} | 142.8 | 24.1 | 0.35 | 119.0 | 15.6 | 0.08 | 182.6 | 20.9 |
| SMP 7 ........... | 3–6 | 137.0 | 53.5 | 110.2 | 29.5 | 1.30 | 151.1 | 43.2 | ... | ... | ... |
| SMP 11 .......... | 1–2 | 130.3 | 17.8 | 129.3 | 19.5 | (0.05 | 158 | 13.7) | ... | ... | ... |
| SMP 14 .......... | 6 | 180.0 | 48.9 | 165.1 | 36.5 | 0.85 | 199.1 | 33.6 | ... | ... | ... |
| SMP 27 .......... | 3 | 101.5 | {19.8, 42.9} | 101.6 | 21.8 | 0.08 | 74.0 | 16.7 | 0.07 | 129.6 | 16.6 |
| SMP 28 .......... | 8 | 176.4 | 54.4 | 183.0 | 34.3 | 0.18 | 146.9 | 43.5 | ... | ... | ... |
| MG 12 ........... | 8 | 111.5 | 47.5 | 111.5 | 52.1 | (1.5 | 98.1 | 6.0) | ... | ... | ... |

NOTE.—Velocities in km s$^{-1}$.
[a] SMP = Sanduleak, McConnell, and Phillip 1978; MG = Morgan and Good 1985.
[b] Excitation class from Morgan 1984.
[c] Height with respect to principal component, corrected for instrumental response function.

the full width at one-tenth maximum, accounting for the difference in strength of the two components.

For those objects fitted by three components, two values of $V_{exp}$ are given.

IV. THE KINEMATICS OF THE PLANETARY POPULATION

The most striking feature of the results presented in the previous section, as far as the kinematics is concerned, is that the PN population of the SMC appears to be completely disordered.

In Figure 2 we plot the spatial distribution of the Sanduleak, McConnell, and Philip (1978) objects with the two genuine Sanduleak and Pesch (1981) PNs and the newly discovered Morgan and Good (1985) identifications. This should result in a fairly uniform magnitude-limited sample covering the whole SMC. The Jacoby (1980) objects have not been used since they are the results of a spatially restricted survey. The 42 PNs form a very loose and extended structure, without a very strong central condensation. However, the centroid of the distribution at $\alpha 00^h49^m30^s$; $\delta -73°20'$ (1950) agrees very closely in position

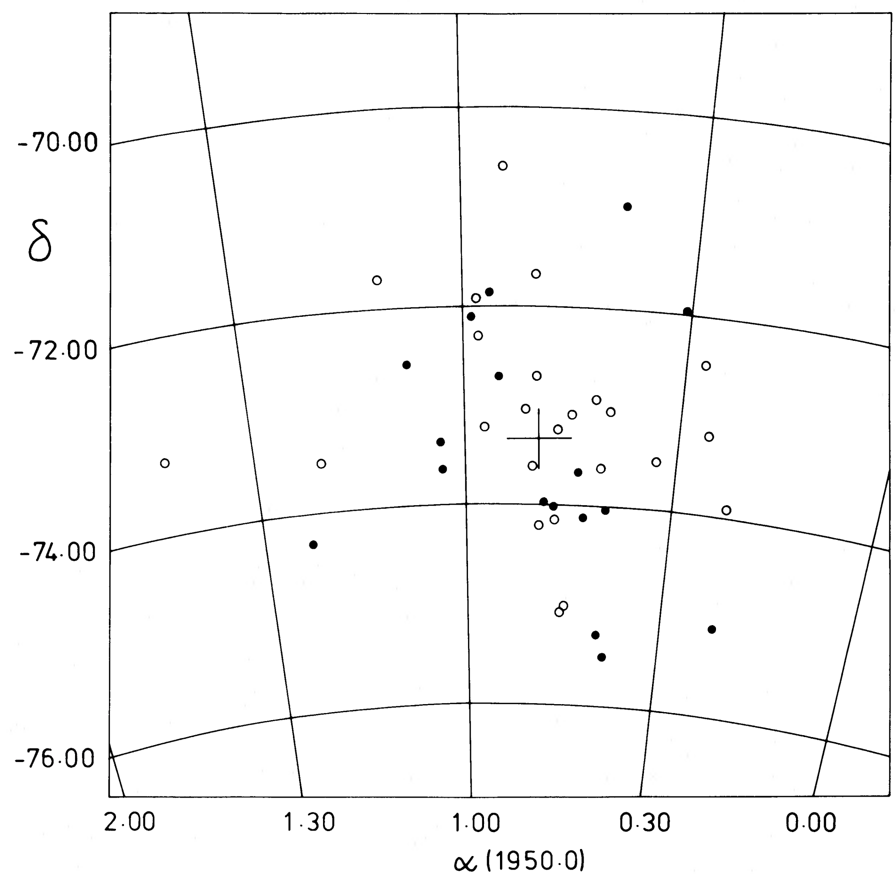


FIG. 2.—The spatial distribution of the SMC planetaries, the Jacoby (1980) objects being excluded. Filled points are planetaries with velocities greater than 140 km s$^{-1}$ ($V_{LSR}$), whereas the open circles represent objects with velocity less than or equal to 140 km s$^{-1}$.

with the brightest region of the SMC Bar and the major axis aligned in a northeast-southwest direction also agrees with that of the Bar.

The impression given by Figure 2, that we are dealing with a spheroidal population, is supported by Figure 3 in which we have plotted the number of PNs in bins of projected distance along the major axis. On such a figure an isothermal distribution with space density $\rho = A/r^2$ should give a surface density $S = \alpha/R_{\text{proj}}$. This is a satisfactory approximation to the observed density bearing in mind that the effects of dust and confusion will reduce the number detected on objective prism surveys close the core of the cloud.

There is very little evidence that this spheroidal population has any organized rotation. In Figure 4 we plot the observed velocity, corrected to Galactocentric standard of rest, $V_{\text{GSR}}$ (on the assumption of a circular rotation in the solar neighborhood of 250 km s$^{-1}$), against the projected distance along the major axis. Not only does this diagram show a lack of rotation (if there is any, it is in the opposite sense to the H I), but it also shows that the dispersion in velocity is effectively independent of position. We do not have any evidence of the bimodal distribution in velocities suggested by Feast (1968) on the basis of observations of 13 PN. Since this may be lost in projection

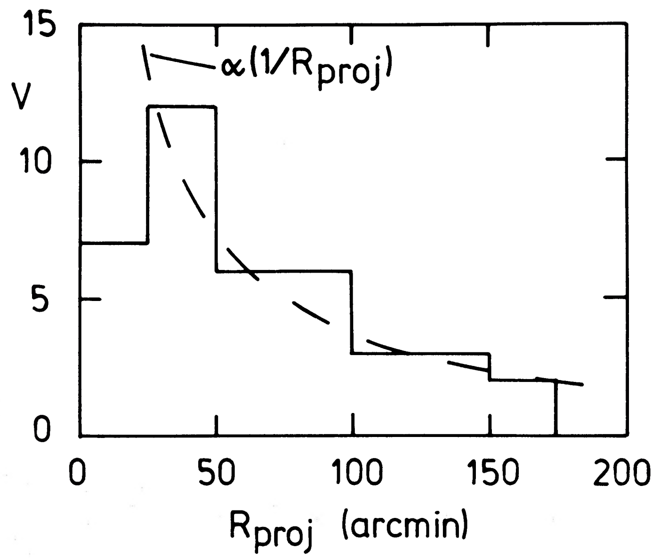


FIG. 3.—The space density of planetaries projected along the major axis of the distribution (NE–SW). The dashed line is a best fit $1/R$ density law.

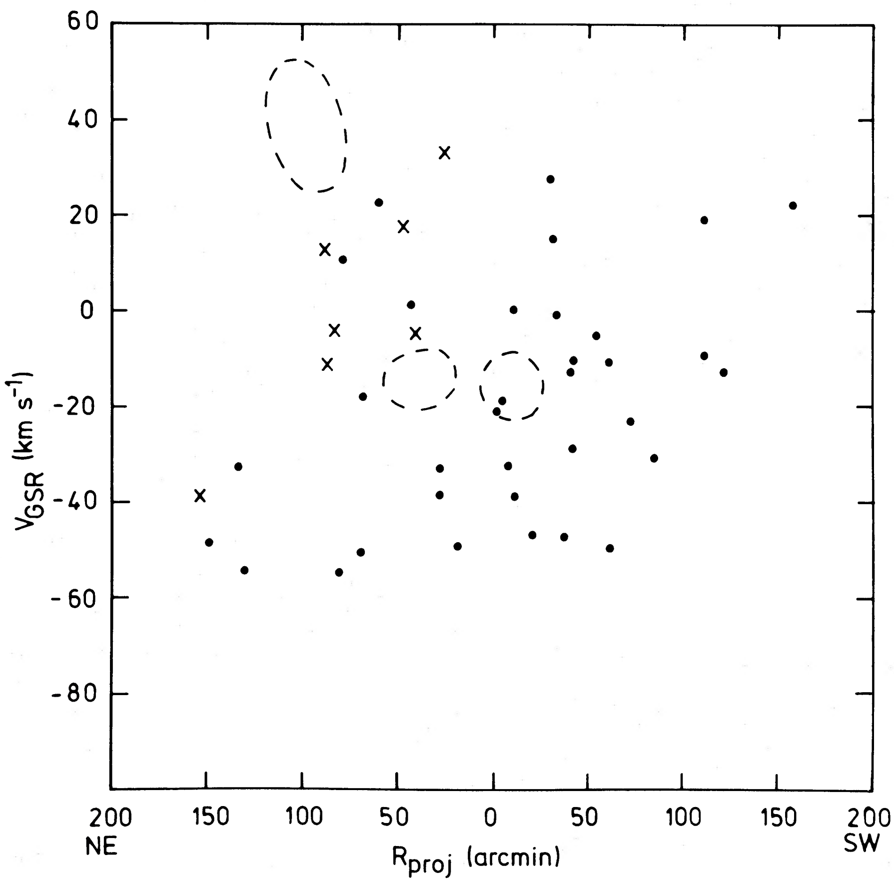


FIG. 4.—The observed galactocentric standard of rest velocity ($V_{\text{GSR}}$) plotted against the projected distance from the centroid along the major axis. This figure is analogous to Fig. 4 of Mathewson and Ford (1984), and we have plotted the principal maxima in the H I distribution as dashed lines. Note the lack of organized rotation and the almost constant velocity dispersion in the planetary population. The crosses represent the apparently younger population of planetaries discussed in the text.

effects on Figure 4, we have tested for a local velocity splitting by plotting a histogram of the modulus of the radial velocity difference between any PN and its (projected) two nearest neighbors (Fig. 5). If the PNs show any tendency to fall into two separate velocity groups, then, even in the presence of strong velocity gradients, such a plot would give a peak near zero and a second peak at the velocity separation of the two components. No such structure is apparent.

There is some evidence for a younger, high-velocity subpopulation of PNs concentrated in the northeast sector of the SMC. These are objects with rather low [O III]/H$\beta$ ratios but very high He II/H$\beta$ ratios which Morgan (1984) found difficult to classify by excitation. A spectroscopic examination (M. A. Dopita, D. H. Morgan, and S. Meatheringham, in preparation) shows that these objects are either dense Peimbert type I objects, or else bright density-limited objects and/or symbiotic stars. These characteristics can be interpreted in terms of relatively massive central stars and stellar precursors. These objects are shown as crosses on Figure 4, to distinguish them from the rest, marked as filled circles, and cluster in a well defined region of higher than average radial velocity all in the northeast part of the SMC. Wood, Bessell, and Fox (1983) argue that the most massive asymptotic giant branch precursors of the planetaries in the Clouds had an initial mass of $\sim 4.9\ M_\odot$ which gives an age of $\gtrsim 7.5 \times 10^7$ yr for the youngest PN population. Thus, the presence of this concentration of young PNs in the northeast of the LMC suggests the presence of a dynamically young region of recent star formation. This region must therefore have an age comparable to or somewhat longer than the age limit given above, say $\lesssim 10^8$ yr.

A comparison with the H I kinematics is instructive. Our Figure 4 is analogous to Figure 4 of the paper by Mathewson and Ford (1984) which shows the results of the 21 cm survey. To assist comparison, we have marked on our Figure 4 the principal maxima seen in the H I. The mean velocity of the complete system of PNs, $V_{\rm GSR} = -18.3$ km s$^{-1}$, agrees fairly well with the mean velocity of the lower velocity H I maxima,

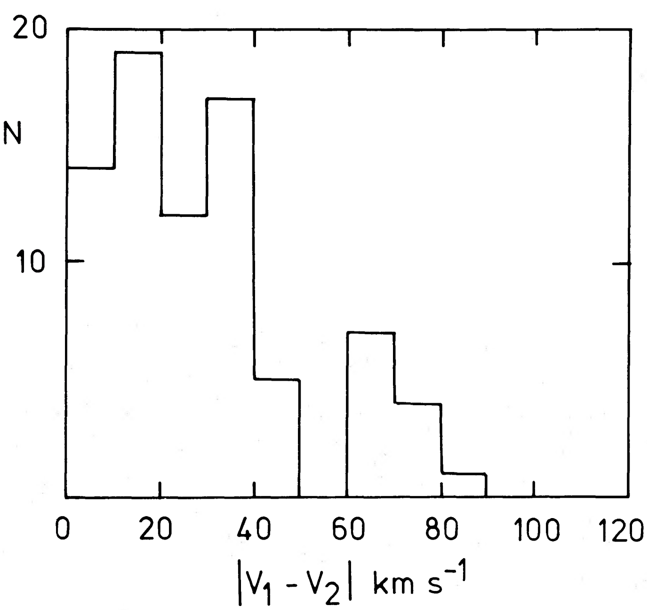


FIG. 5.—A histogram of the modulus of the radial velocity difference between any planetary and its two nearest neighbors in projection. No sign of a bimodal distribution is apparent.

about $V_{\rm GSR} = -15$ km s$^{-1}$. If only the older PNs are considered, the mean velocity is somewhat lower still: $V_{\rm GSR} = -22$ km s$^{-1}$. Furthermore, many have velocities in the range $-50$ to $-60$ km s$^{-1}$, which is outside the range of all but a faint tail of H I. A few PNs also appear in projection beyond the limits of the main body of H I in the northwest region of the SMC. Thus, in summary, the older PN system forms a disorganized structure which is closely associated with the SMC Bar population of older stars and which is associated with, but somewhat displaced from, the low-velocity H I gas. However, this gaseous component has a more organized structure and a lower velocity dispersion, indicating that dissipational processes have operated on it.

The spatial location and velocity distribution of the younger planetary subsystem is significantly different and highly suggestive. They cluster in a region of the SMC that is certainly associated with a young stellar population (Mathewson and Ford 1984 and references therein). Although their mean velocities ($V_{\rm GSR} = +0.2$ km s$^{-1}$) are not as great as the high velocity H I concentration, they are nevertheless more clearly associated with this than the low-velocity H I gas. The impression from Figure 4 is that the young PNs have been shed from this H I gas at an earlier epoch.

Azzopardi (1982) has measured the distance modulii of the A, B, and O supergiants in the SMC. They find not only do these have an appreciable spread in distance modulus, corresponding to a spatial depth of order 7 kpc, but the younger stars have an appreciably larger distance modulus on the mean and concentrate in the northeast sector. The total depth of the SMC also appears to be largest in this sector. These results are consistent with an armlike gaseous feature moving away from both us and the core of the SMC, continually forming stars as it goes. The younger subsystem of planetaries (which are still older than the supergiants) are in the region of the "arm" closest to the central body which contains the older PN. Given the difference in velocity between this feature, $V_{\rm GSR} = +45$ km s$^{-1}$, and the mean for the SMC planetaries, $V_{\rm GSR} = -17$ km s$^{-1}$, then in $10^8$ yr, the arm will have moved (in depth) by some 6 kpc, in good agreement with the 7 kpc quoted above.

Thus, we agree with Mathewson and Ford (1984) that the SMC appears to have been disrupted by tidal forces in the recent past, probably by a near collision with the LMC (Murai and Fujimoto 1980; Fujimoto and Murai 1984). However, the PN data shows that the effect of this has been quite different on the older stellar component and on the gas. The stellar component is roughly spheroidal, whereas the gaseous component has developed a tidal counterarm moving away from us. Since the velocity splitting is continuous into the intercloud, this presumably indicates that both tidal arm and counterarm are on the same line of sight. A physical separation of the gaseous and stellar components requires that shocks were formed in the former with velocities of order of the separation of the components: 40–50 km s$^{-1}$, indicating a fairly severe encounter. This could have occurred either in a direct collision between the SMC and LMC disks or else by a sufficiently severe tidal torquing of an earlier SMC disk to produce retrograde or crossing orbits.

Finally, we use the rms line-of-sight velocity dispersion, $\langle V_Z{}^2 \rangle^{1/2}$, observed for the PNs; 25.3 km s$^{-1}$, to derive a total mass of the SMC within 150″ (3 kpc) and assuming that the planetary nebulae are test particles with two degrees of freedom; in which case $M(R) = 2\langle V_Z{}^2 \rangle R/G$. This gives a mass of $9 \times 10^8\ M_\odot$ within $R = 3$ kpc. The mass derived by

Hindman (1967) from the H I was higher, $1.5 \times 10^9$ $M_\odot$, but this was derived on the interpretation of the H I motions as due to rotation, which, as we have seen, is probably not the case. We regard the mass estimate given by the planetaries as more reliable. Since roughly half of the H I is associated with the spheroidal component, the value of the hydrogen to total mass ratio is about 0.27.

## V. THE INTERNAL DYNAMICS OF THE SMC PLANETARY NEBULAE

In an ideal world, we would like to compare the expansion velocities we observe with the other properties of the planetary such as luminosity, temperature and mass of the central star and nebular diameter. However, currently no such information is available for the whole sample and even the spectrophotometry published in the literature is fragmentary. The largest sample is by Aller *et al.* (1981) who observed SMP 2, 15, 17, 24, and 27. Osmer (1976) observed SMP 2, 20, and 22, and Dufour and Killen (1977) and Webster (1978) also observed SMP 22. M. A. Dopita, D. H. Morgan, and S. Meatheringham (in preparation) have spectrophotometry on SMP 7, 22, 25, and 26 and MG 13.

Morgan (1984) has given excitation classification for all the SMP objects, and these are listed in Tables 3 and 4. In Figure 6, we have plotted the expansion velocity against the excitation class. On this figure, double component objects are plotted as open circles. A remarkably good positive correlation is evident. Without further information, we cannot fully elucidate the reason for this, but we can make some progress by considering the selection effect in the sample.

The SMC sample is effectively an H$\beta$ flux-limited sample at constant distance. Since, in an optically thick nebula, each UV photon is absorbed in the nebula and the number of photons produced by the central star balances the number of recombinations, the H$\beta$ flux is a measure of the UV luminosity, which for temperatures in excess of about 30,000 K can be roughly equated with the bolometric luminosity of the central star. Thus, the planetary nebula sample is complete in the H-R diagram down to some limiting stellar luminosity.

The excitation class depends largely on effective temperature, but also on the ionization parameter in the nebula, roughly defined as the number of ionizing photons per hydrogen atom averaged throughout the nebula.

However, the density is correlated with the physics of the ejection and acceleration process. For galactic PNs, a variety of models have been advanced to explain the radius/expansion velocity correlation (which is largely absent at radii $\gtrsim 0.1$ pc; Chu *et al.* 1984). It is not clear to us whether a "two-wind" (Mathews 1966; Kwok *et al.* 1978; Kwok 1982) or a "two-phase" (Sabbadin *et al.* 1984) or other models such as those recently discussed by Phillips (1984) are appropriate or complete representations of reality. In particular, we have little understanding of how any of these variables depend on the mass of the central star. We therefore cannot be sure if a line of constant excitation parameter tracks to the left or the right of a line of constant stellar temperature as we move to higher stellar luminosity in the H-R diagram. However, we are sure that high-mass, high-luminosity nuclei are rather unlikely to be seen at low effective temperatures. This is because theoretical models show very rapid evolution across this part of the H-R diagram (Paczyński 1971), even when the phase of the helium

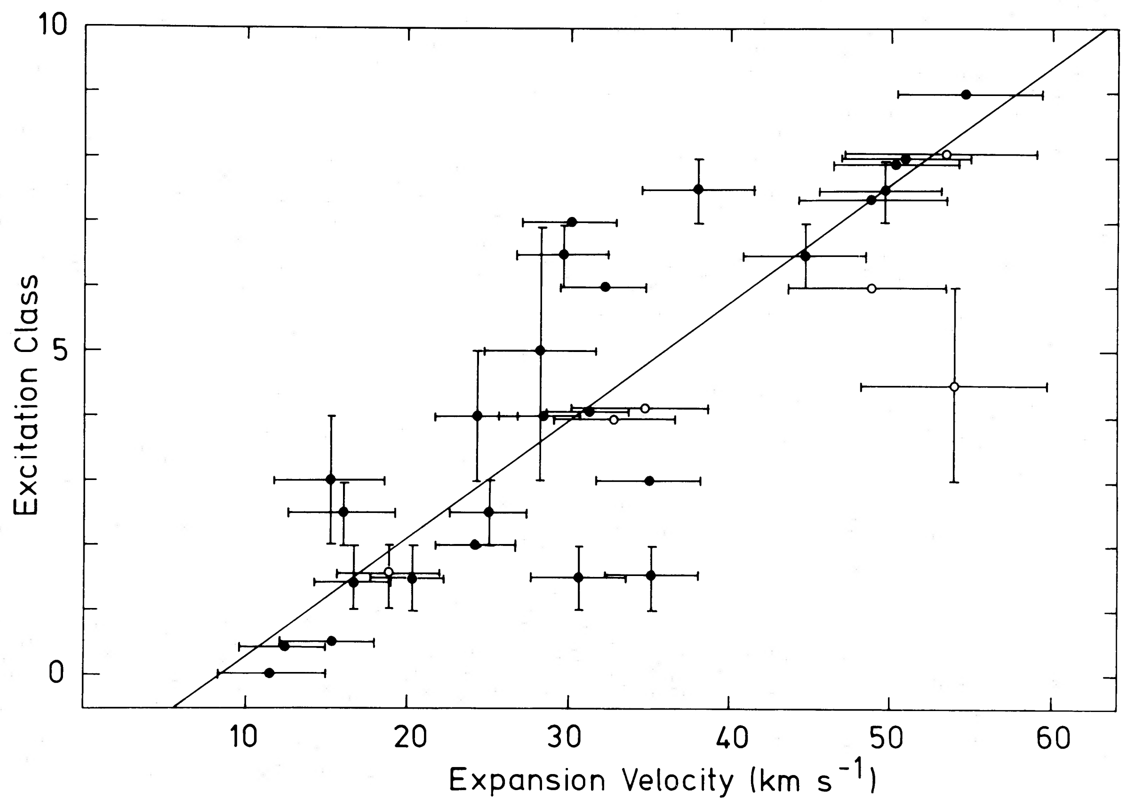


FIG. 6.—The expansion velocity of the planetaries as a function of excitation class. Open circles represent double component planetaries, and the line is the linear regression fit which crosses excitation class 0 at 8 km s$^{-1}$, very close to what is thought to be the expansion velocity of red giant winds.

shell flash is taken into account (Wood and Faulkner 1984). Furthermore, because of the flux limit in our sample, objects with a stellar luminosity less than $\sim 10^3 L_\odot$ will be infrequent.

From these selection effects, we conclude that objects of a given excitation class have central stars of similar effective temperatures; that the mean luminosity within an excitation class differs little from one excitation class to the next (this is observed by Morgan 1984); and finally, from the shape of the theoretical evolution tracks, that a given excitation class *in this sample* is related to the mass of the central star. Figure 6 is therefore interpreted as a relationship between expansion velocity and mass of the white dwarf nucleus. This hypothesis is supported by the fact that the "young" planetaries identified in the previous section have noticeably larger expansion velocities than the mean (Fig. 7). If we are correct, then the fact that high-mass nuclei produce rapidly expanding nebulae (despite the very short time scales available for acceleration of a nebular shell in the PN phase) suggests that either acceleration of the nebula is very large or that the expansion velocity reflects that of an initial ejection process such as in the two-phase model of Sabbadin *et al.* (1984).

This intriguing result is only provisional and requires further observational support. It is possible that, below excitation class 3, our [O III] expansion velocity is not measuring the expansion velocity at the ionization front which may be larger (Chu *et al.* 1984). We are therefore reobserving many of these and higher excitation nebulae in the [O II] doublet to give both this information and the density information required to help estimate the ionization parameter. Some of us also are conducting a program of absolute photometry to give the luminosity data and also a program of speckle interferometry to furnish diameter information. With this data we expect to be able to give important new observational constraints of the physics of planetary nebula ejection.

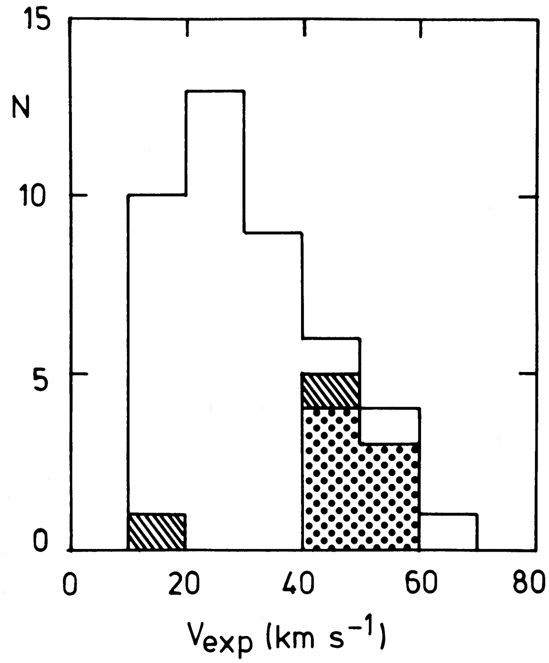


FIG. 7.—A histogram of expansion velocity. Dot shaded sections represent the young planetaries identified in the text, and dash shaded sections are suspected members.

One of us (H. C. F.) would like to thank the Australian National University for the support of a Visiting Fellowship during the period in which many of the observations described in ths paper were made.

REFERENCES


Aller, L. H., Keyes, C. D., Ross, J. E., and O'Mara, B. J. 1981, *M.N.R.A.S.*, **194**, 613.
Azzopardi, M. 1982, in *Comptes Rendus sur les Journèes de Strasbourg* (Strasbourg: Observatoire de Strasbourg), p. 20.
Bajaja, E., and Loiseau, N. 1982, *Astr. Ap. Suppl.*, **48**, 71.
Bohuski, T. J., and Smith, M. J. 1974, *Ap. J.*, **193**, 197.
Boksenberg, A. 1972, in *Proc. ESO/CERN Conf. on Auxiliary Instrumentation for Large Telescopes*, ed. S. Lansten and A. Reiz (Geneva: ESO/CERN), p. 295.
Chu, Y.-H., Kwitter, K. B., Kaler, J. B., and Jacoby, G. H. 1984, *Ap. J.*, submitted.
Dufour, R. J. and Killen, R. M. 1977, *Ap. J.*, **211**, 68.
Feast, M. W. 1968, *M.N.R.A.S.*, **140**, 345.
Fujimoto, M., and Murai, T. 1984, in *Structure and Evolution of the Magellanic Clouds*, ed. S. van den Bergh and K. S. de Boer (Dordrecht: Reidel), p. 115.
Henize, K. G. 1956, *Ap. J. Suppl.*, **2**, 315.
Henize, K. G., and Westerlund, B. E. 1963, *Ap. J.*, **137**, 747.
Hindman, J. V. 1967, *Australian J. Phys.*, **20**, 147.
Iben, I. 1981, *Ap. J.*, **246**, 278.
Jacoby, G. H. 1980, *Ap. J. Suppl.*, **42**, 1.
Kwok, S. 1982, *Ap. J.*, **258**, 280.
Kwok, S., Purton, C. R., and Fitzgerald, P. M. 1978, *Ap. J. (Letters)*, **219**, L125.
Lindsay, E. M., and Mullen, D. J. 1963, *Irish Astr. J.*, **6**, 51.
Mathews, W. G. 1966, *Ap. J.*, **143**, 173.
Mathewson, D. S., and Ford, V. L. 1984, in *IAU Symposium 108, Structure and Evolution of the Magellanic Clouds*, ed. S. van den Bergh and T. S. de Boer (Dordrecht: Reidel), p. 125.
McGee, R. X., and Newton, L. M. 1981, *Proc. Astr. Soc. Australia*, **4**, 189.
Morgan, D. H. 1984, *M.N.R.A.S.*, **209**, 241.
Morgan, D. H., and Good, A. 1985, *M.N.R.A.S.*, in press.
Murai, T., and Fujimoto, M. 1980, *Pub. Astr. Soc., Japan*, **32**, 581.
Osmer, P. S. 1976, *Ap. J.*, **203**, 352.
Paczyński, B. 1971, *Acta Astr.*, **21**, 271.
Pelat, D., Alloin, D., and Fosbury, R. A. E. 1981, *M.N.R.A.S.*, **195**, 787.
Phillips, J. P. 1984, *Astr. Ap.*, **137**, 92.
Robinson, G. J., Reay, N. K., and Atherton, P. D. 1982, *M.N.R.A.S.*, **199**, 649.
Sabbadin, F., Bianchini, A., and Hamzaoglu, E. 1984, *Astr. Ap.*, **136**, 200.
Sabbadin, F., Gratton, R. G., Bianchini, A., and Ortolani, S. 1984, *Astr. Ap.*, **136**, 181.
Sabbadin, F., and Hamzaoglu, E. 1982, *Astr. Ap.*, **110**, 105.
Sanduleak, N., McConnell, D. J., and Philip, A. G. D. 1978, *Pub. A.S.P.*, **90**, 621.
Sanduleak, N., and Pesch, P. 1981, *Pub. A.S.P.*, **93**, 431.
Smith, H. C. 1969, M.A. thesis, University of Virginia.
Stapinski, T. E., Rodgers, A. W., and Ellis, M. J. 1981, *Pub. A.S.P.*, **93**, 242.
Webster, B. L. 1969, *M.N.R.A.S.*, **143**, 97.
———. 1978, in *IAU Symposium 76, Planetary Nebulae*, ed. Y. Terzian (Dordrecht: Reidel), p. 11.
Wood, P. R., Bessell, M. S., and Fox, M. W. 1983, *Ap. J.*, **272**, 99.
Wood, P. R., and Faulkner, D. J. 1984, in *Observational Tests of the Stellar Evolution Theory*, ed. A. Maeder and A. Renzini (Dordrecht: Reidel), p. 179.



MICHAEL A. DOPITA and CATHERINE J. LAWRENCE: Mount Stromlo and Siding Spring Observatories, Private Bag, Woden P.O. ACT 2606, Australia

HOLLAND C. FORD: Space Telescope Science Institute, Homewood Campus, Baltimore, MD 21218 U.S.A.

B. LOUISE WEBSTER: School of Physics, University of New South Wales, P.O. Box 1, Kensington N.S.W. 2033, Australia